

Calculation of the Volumetric Heat Generation Rate Radial Profile in a Cylindrical Fuel Rod

by

V.I. Arimescu, M. Couture, M.E. Klein and A.F. Williams
AECL
Chalk River Laboratories
Fuel Safety Branch

1. INTRODUCTION

Since most of the physical processes occurring in UO_2 have a thermally activated component, an accurate temperature calculation is needed for their correct estimation. The thermal analysis in a fuel rod is governed by the heat conduction equation. One of the terms in this equation is the local heat generation rate whose modeling is the object of this paper.

In the present versions of ELESIM/ELESTRES [1-2], the radial profile of the heat generation rate is modeled by a three parameter correlation. Two databases exist for these parameters. Both were established by using the reactor physics code CE-HAMMER to calculate the local heat generation rate for fuel pins of various radii, enrichment and burnup. The original database included fuel burnups in the range 0 to 480 MWh/kgU. The most recent database is an extension to burnups of 840 MWh/kgU. There exist, however, inconsistencies between the two databases that need to be resolved.

This motivated us to develop a new code, RAD_HEAT, whose evaluation of the local heat generation rate is based on a more mechanistic approach that does not rely on these databases. Two factors that contribute to changes in the heat generation are the thermal neutron flux depression due to self-shielding, and a non-uniform buildup of Pu^{239} . The radial profile of Pu^{239} varies with burnup and is characterized, at high burnup, by a sharp increase in the concentration near the surface of the pellet. This non uniform distribution is due to the resonance capture of epithermal neutrons by U^{238} . In RAD_HEAT, our modeling of resonance capture phenomenon is based on Wagner's work [3] which considers the fuel element as a pure absorber. Several input parameters, such as the cross sections, are evaluated with WIMS-AECL. It is intended that RAD_HEAT be incorporated in ELESIM/ELESTRES.

The paper is organized as follows. In Section 2, the relative power density factors are defined. A model for resonance capture in U^{238} is described in Section 3. In Section 4, a set of depletion equations and their solutions are presented. Finally, test cases are discussed in Section 5.

2. RELATIVE POWER DENSITY FACTORS

In RAD_HEAT, the radial profile of the heat generation rate is calculated by dividing the fuel into a number n_{an} of annuli and solving, for each annulus J , the power density H^J . The local heat generation rate $H^J(t)$ in annulus J and at time t is defined as

$$H^J(t) = \alpha_f \eta_{ff} \Phi_{ther}^J \sum_k N_k^J(t) \sigma_k^f \quad \text{for } J=1, n_{an} \quad (2.1)$$

where α_f is the energy release per fission (≈ 200 MeV), η_{ff} is the U^{238} fast fission factor (1.08), Φ_{ther}^J is the time and volume-averaged thermal neutron flux in annulus J , $N_k^J(t)$ is the volume-averaged concentration of fissile nuclei k ($k = 1$ for U^{235} , $k = 2$ for Pu^{239}) in annulus J and at time t , and σ_k^f is the time and volume-averaged weighted fission cross section of nuclei k . The time-averaged radial distribution $\Phi_{ther}(r)$ of the thermal flux within the pellet is assumed to be a solution of the one dimensional diffusion equation. For a solid pellet

$$\Phi_{ther}(r) = I_0(\kappa r) \quad 0 \leq r \leq R_{pin}$$

where I_0 is the modified Bessel function of the first kind and of order zero, R_{pin} is the radius of the pin and κ is the inverse of the thermal diffusion length. The value of κ is obtained by fitting $\Phi_{ther}(r)$ to the thermal fluxes (for various burnups) calculated with WIMS-AECL. The time and volume-averaged thermal flux Φ_{ther}^J within annulus J of the fuel pin is then equal to

$$\Phi_{ther}^J = \frac{2 \int_{r_{in}}^{r_{out}} \Phi_{ther}(r) r dr}{(r_{out}^2 - r_{in}^2)} \quad (2.2)$$

where r_{in} and r_{out} are the inner and outer radius of annulus J . This approach can be easily extended to include pellets with a central hole. The volume-averaged heat generation rate $\bar{H}(t)$ in the pin at time t is then equal to

$$\bar{H}(t) = \frac{\sum_J H^J(t)V^J}{\sum_J V^J}$$

where V^J is the volume of annulus J . The relative power density factors $\Gamma^J(t)$ are defined as

$$\Gamma^J(t) \equiv \frac{H^J(t)}{\bar{H}(t)} \quad \text{for } J=1, n_{an}. \quad (2.3)$$

In Section 5 we compare power density factors calculated by RAD_HEAT and with those calculated by ELESIM/ELESTRES. The fission cross sections in equation (2.1) are obtained through a WIMS-AECL calculation. The concentrations are the only remaining unknowns in equation (2.1). They can be obtained by solving a set of depletion equations, the formulation of which requires a model for the radial profile of the resonance capture rate in U^{238} .

3. A MODEL FOR THE LOCAL RESONANCE CAPTURE RATES IN U^{238}

Wagner [3] gives formulas for the rate of resonance capture per unit volume at any point within an infinite cylindrical solid fuel pin due to a single well-resolved resonance of the Breit-Wigner type. An important feature of his model is that for most points within the fuel the radial distribution of resonance capture is expressed as a universal function independent of the resonance parameters. Comparisons [3] with experimental data published by Hellstrand [4] strongly suggest that this function could be a good approximation for the radial profile of the total (all resonances) capture rate. We shall first describe Wagner's model and then address the issue of how it is implemented in the code RAD_HEAT.

Wagner's model [3] is based on the following four assumptions:

- The fuel pellet is solid, cylindrical and of infinite length.
- The moderator's epithermal neutron flux is homogeneous and isotropic with an $1/E$ energy dependence.
- Scattering within the fuel can be neglected, making the fuel a pure absorber.
- The Doppler broadening of the resonance can be neglected and only resonances of the Breit-Wigner type need be considered.

Let R_{pin} denote the radius of the pellet and consider some arbitrary point P_0 located at a radial distance $r \leq R_{pin}$ from the axis of the pellet. Since the fuel is a pure absorber, depletion of the epithermal flux only occurs through resonance captures. The energy dependent epithermal flux Φ_{epi} at point P_0 is therefore given by

$$\Phi_{epi}(r, \xi) = \frac{S^*}{2\pi E_0} \int_A e^{-D\Sigma(\xi)} d\Omega \quad ; \quad \Sigma(\xi) = \frac{\Sigma_0}{1 + \xi^2}$$

where $\Sigma(\xi)$ is the macroscopic resonance cross section at energy E and

$$\xi = \frac{2(E - E_0)}{T}$$

where Σ_0 is the macroscopic cross section at resonance energy E_0 and T the total line width of the resonance. The factor $S^*/2\pi E_0$ represents (S^* is a source term) the epithermal angular neutron flux which enters the fuel element at some arbitrary point

Q_1 and whose direction is that of the vector $\vec{Q_1 P_0}$. D is the distance between points Q_1 and P_0 . $d\Omega$ is a solid angle subtended at point P_0 by an element of surface about point Q_1 . The total epithermal flux (at energy E) at P_0 is then obtained by adding (integrating over $d\Omega$) the contribution from all points on the surface A of the cylinder (end caps are neglected since we are dealing with an infinite cylinder). $W(r)$, the rate of resonance capture per unit volume at point P_0 , is therefore

$$W(r) = \frac{\Gamma}{2} \int_{-\infty}^{\infty} \Phi_{epi}(r, \xi) \Sigma(\xi) d\xi \quad (3.1)$$

When $R_{pin} - r \gg 1/\Sigma_0$ or $R_{pin} - r \approx 1/\Sigma_0$, one can use the asymptotic expansion of I_0 to simplify the evaluation of the integral in equation (3.1). For the region well within the fuel

$$W(r) \approx \frac{.874\pi \Sigma_0 T S^*}{E_0 \sqrt{\pi \Sigma_0 R_{pin}}} f(r/R_{pin}) \quad \text{for } R_{pin} - r \gg 1/\Sigma_0 \quad (3.2)$$

where

$$f(r/R_{pin}) = F\left(\frac{5}{4}, \frac{5}{4}, 1; (r/R_{pin})^2\right) - \frac{5}{4} (r/R_{pin})^2 F\left(\frac{5}{4}, \frac{9}{4}, 2; (r/R_{pin})^2\right)$$

and F is the hypergeometric series. Note that in this case, the radial distribution function $f(r/R_{pin})$ is independent of the parameters of the resonance. It is therefore a universal function valid for all resonances. For P_0 in the vicinity of the surface one gets

$$W(r) \approx \frac{\Sigma_0 T S^*}{2E_0} \left[\pi G\left(\Sigma_0 (R_{pin} - r)/2\right) + \frac{1.8285}{\sqrt{\Sigma_0 R_{pin}}} \right] \quad \text{for } R_{pin} - r \approx 1/\Sigma_0 \quad (3.3)$$

where

$$G(\lambda) = \int_0^{\infty} \frac{e^{-\lambda t} I_0(\lambda t)}{t^2} dt.$$

In this case the radial distribution is no longer independent of the parameters of the resonance. We conclude this outline of Wagner's results by stressing the fact that the results given in equations (3.2) and (3.3) are resonance capture rates due to a single resonance. Nevertheless, since for most points in the fuel the radial dependence of the resonance capture rate is expressed in terms of a universal function, we might expect, as Wagner's comparison [3] with Hellstrands's [4] experimental data suggests, the same radial dependence for the total capture rate.

The strategy used in the code RAD_HEAT to model the *total* resonance capture rate is therefore as follows. The resonance dependent parameters in equations (3.2) and (3.3) are removed by normalization (we are only interested in ratios of resonance capture rates, see equation (3.4)) and by replacing Σ_0 with Σ_{av} , which can be regarded as an average resonance cross section. The fuel pin is divided into three regions. Regions 1 and 3 are chosen so that the radial dependence of equations (3.3) and (3.2) can be applied. The functional form of region 2 is chosen so that there is a smooth transition. The total resonance capture rate $C_{tot}(r)$ at point P_0 is described by one of the following functions

$$C_3(r) = f\left(r/R_{pin}\right) \quad \text{for} \quad R_{pin} - r > \frac{25}{\Sigma_{av}}$$

$$C_2(r) = 0.2 \Sigma_{av} \left[\mu_1 f\left(r/R_{pin}\right) - \mu_2 W_2\left(R_{pin} - r\right) \right] \quad \text{for} \quad \frac{20}{\Sigma_{av}} < R_{pin} - r \leq \frac{25}{\Sigma_{av}}$$

$$C_1(r) = \frac{\sqrt{\pi \Sigma_{av} R_{pin}}}{1.748 \pi} W_2\left(R_{pin} - r\right) \quad \text{for} \quad R_{pin} - r \leq \frac{20}{\Sigma_{av}}$$

where

$$W_2\left(R_{pin} - r\right) = \left[\pi G\left(\Sigma_{av}\left(R_{pin} - r\right)/2\right) + \frac{1.8285}{\sqrt{\Sigma_{av} R_{pin}}} \right]$$

$$\mu_1 = R_{pin} - r - \frac{20}{\Sigma_{av}} \quad ; \quad \mu_2 = \frac{\sqrt{\pi \Sigma_{av} R_{pin}}}{1.748 \pi} \left(R_{pin} - r - \frac{25}{\Sigma_{av}} \right).$$

The model depends on the free parameter Σ_{av} which can be determined by comparing code predictions and experimental data (see Section 5).

In the code RAD_HEAT, the fuel pin is divided into several annuli and the above model is used to calculate the volume-averaged rate of resonance captures in each annulus J and in the pin

$$C_{tot}^J = \frac{\int_C C_{tot}(r) r dr}{\int_J r dr} ; C_{tot}^{pin} = \frac{\int_{pin} C_{tot}(r) r dr}{\int_{pin} r dr} .$$

The rate of resonance capture for the case of a pin with a hole is assumed to be identical to that of a pin with no hole. For each annulus the following ratio is defined for use in modeling the resonance capture term in the depletion equations

$$\Lambda^J = \frac{C_{tot}^J}{C_{tot}^{pin}} \quad \text{for } J=1, n_{an}. \quad (3.4)$$

4. DEPLETION EQUATIONS

Since the percentage of depletion of U^{238} is small, we consider its concentration as constant throughout burnup and denote it \bar{N}_{238} . The fuel is divided into a number n_{an} of annuli and the depletion equations are formulated and solved for each annulus

$$\frac{dN_{235}^J(t)}{dt} = -\sigma_{235}^a N_{235}^J(t) \Phi_{ther}^J \quad \text{for } J=1, n_{an} \quad (4.1)$$

$$\begin{aligned} \frac{dN_{239}^J(t)}{dt} = & -\sigma_{239}^a N_{239}^J(t) \Phi_{ther}^J + \sigma_{238,res}^c \bar{N}_{238} \Phi_{epi}^J + \sigma_{238,ther}^c \bar{N}_{238} \Phi_{ther}^J \\ & + \sigma_{238,fast}^c \bar{N}_{238} \Phi_{fast}^J \quad \text{for } J=1, n_{an} \quad (4.2) \end{aligned}$$

where $N_k^J(t)$ is the volume-averaged concentration for nuclei k ($k=235$ for U^{235} and $k=239$ for Pu^{239}) in annulus J at time t . Φ_{epi}^J and Φ_{fast}^J are respectively the time and volume-averaged epithermal and fast fluxes in annulus J . $\sigma_{238,res}^c$, $\sigma_{238,ther}^c$ and $\sigma_{238,fast}^c$ are the time and volume-averaged weighted resonance, thermal and fast capture cross sections of U^{238} . Finally, σ_{235}^a and σ_{239}^a are the time and volume-averaged weighted absorption cross sections of U^{235} and Pu^{239} .

All the cross sections can be evaluated using the reactor physics code WIMS-AECL and the thermal flux is given by equation (2.2). What remains to be specified, in equations (4.1) and (4.2), are the epithermal and fast fluxes. The goal is to express them in terms of the thermal flux. Using the model of resonance capture described in the previous section and equation (3.4),

$$\frac{\Phi_{epi}^J}{\Phi_{epi}^{pin}} = \Lambda^J. \quad (4.3)$$

The ratio of pin-averaged epithermal to thermal flux can then be calculated using WIMS-AECL

$$\beta \equiv \frac{\phi_{epi}^{pin}}{\phi_{ther}^{pin}} \quad (4.4)$$

where the use of ϕ instead of Φ indicates that these are fluxes calculated by the code WIMS-AECL. Combining (4.3) and (4.4) we get

$$\Phi_{epi}^J = \beta \Lambda^J \Phi_{ther}^{pin}. \quad (4.5)$$

A similar strategy is used for the fast flux

$$\zeta_{fast}^J \equiv \frac{\phi_{fast}^J}{\phi_{ther}^J} \Rightarrow \Phi_{fast}^J = \zeta_{fast}^J \Phi_{ther}^J \quad (4.6)$$

where ϕ represents fluxes calculated using WIMS-AECL. The parameters β and ζ_{fast}^J will vary with burnup and fuel type.

The next step consist of formulating the depletion equations in terms of local burnups using the following relations

$$\frac{dbu^J}{dt} = \frac{H^J(t)}{\rho_{fuel}} \quad \text{for } J = 1, n_{an} \quad ; \quad \frac{d\bar{bu}}{dt} = \frac{\bar{H}(t)}{\rho_{fuel}} \quad (4.7)$$

where ρ_{fuel} is the fuel density, bu^J the volume averaged burnup in annulus J , and \bar{bu} the volume-averaged burnup in the pin. Recalling equation (2.1), and combining the results expressed in equations (4.5), (4.6) and the first relation of equation (4.7), one gets

$$\frac{dN_{235}^J(bu^J)}{dbu^J} = -l_0^J N_{235}^J(bu^J) \quad \text{for } J=1, n_{an} \quad (4.8)$$

$$\frac{dN_{239}^J(bu^J)}{dbu^J} = -l_3^J N_{239}^J(bu^J) + (l_1^J + l_2^J + l_4^J) \bar{N}_{238} \quad \text{for } J=1, n_{an} \quad (4.9)$$

where

$$l_0^J = \frac{\sigma_{235}^a \rho_{fuel}}{\eta_{ff} \alpha_f \sum_k N_k^J(bu^J) \sigma_k^f} \quad ; \quad l_1^J = \frac{\beta \Lambda^J \rho_{fuel} \sigma_{238,res}^c}{\eta_{ff} \alpha_f \sum_k N_k^J(bu^J) \sigma_k^f} \frac{\Phi_{ther}^{pin}}{\Phi_{ther}^J}$$

$$l_2^J = \frac{\sigma_{238,ther}^c \rho_{fuel}}{\eta_{ff} \alpha_f \sum_k N_k^J(bu^J) \sigma_k^f}; l_3^J = \frac{\sigma_{239}^a \rho_{fuel}}{\eta_{ff} \alpha_f \sum_k N_k^J(bu^J) \sigma_k^f}; l_4^J = \frac{\sigma_{238,fast}^c \rho_{fuel} S_{fast}^J}{\eta_{ff} \alpha_f \sum_k N_k^J(bu^J) \sigma_k^f}$$

Since the coefficients l_i^J ($i=0, 4$) are functions of the local concentrations, they are burnup dependent. The task of solving these equations is simplified greatly if we seek solutions which are valid for a small local burnup increment $\Delta bu^J = bu_f^J - bu_i^J$. Here bu_i^J and bu_f^J are the initial and final local burnup value. If Δbu^J is small enough, a reasonable approximation is to consider the local power density to be constant during that burnup interval. With such an approximation, the coefficients l_i^J can be considered constants whose values are determined by the concentrations at the initial burnup value bu_i^J . Equations (4.8) and (4.9) then become first order linear differential equations which can be solved by standard methods

$$N_{235}^J(bu_f^J) = N_{235}^J(bu_i^J) \exp(-l_0^J \Delta bu^J) \quad (4.10)$$

$$N_{239}^J(bu_f^J) = \exp(-l_3^J \Delta bu^J) \left[\left(\frac{(l_1^J + l_2^J + l_4^J) \bar{N}_{238}}{l_3^J} \right) (\exp(l_3^J \Delta bu^J) - 1) + N_{239}^J(bu_i^J) \right].$$

In RAD_HEAT, for each global burnup step $\Delta \bar{bu}$ the corresponding local burnup step Δbu^J is evaluated using the following relation

$$\Delta bu^J = \Gamma^J(t_i) \Delta \bar{bu} \quad \text{for } J=1, n_{an}$$

where here $\Gamma^J(t_i)$, given by equation (2.3), is the value of the power density factor in annulus J at the beginning of the burnup step ($\Delta t = t_f - t_i$). The result is then substituted on the right hand side of equation (4.10) to obtain the new concentrations. The process is repeated for each global burnup step.

5. APPLICATION OF RAD_HEAT

Before RAD_HEAT can be applied, a value for the parameter Σ_{an} must be determined. This was done by fitting the total (fast, epithermal and thermal) neutron capture rate in U^{238} predicted by the code RAD_HEAT with experimental data obtained by A. Okazaki, D.W. Hone and D.F. Allen (unpublished data, 1959) at the ZEEP (Zero Energy

Experimental Pile) reactor. The total capture rate in U^{238} is modeled by the second term on the right hand side of equation (4.9).

Neutron capture in U^{238} results in the formation of Pu^{239} . The transformation of U^{238} into Pu^{239} is accompanied by x-ray emissions that can be measured. Okazaki et al. obtained the radial profile of neutron capture in U^{238} by measuring this activity in thin samples taken at various depths of ZEEP rods. The moderator in this experiment was heavy water. Figure 1 and Table 1 show the total capture as predicted by RAD_HEAT (a burnup of 0 is assumed) and as measured by Okazaki et al. for a natural uranium metal rod of 3.26 cm in diameter with an aluminum cladding of .1 cm in thickness and a .015 cm gap. The rod was located at the center of the core whose hexagonal lattice had a center-to-center spacing of 5.77 cm. The results are normalized to unity at the point nearest to the surface. In the column 'distance', we give the distance from the longitudinal axis of the rod. Error bars for the experimental data were not provided by Okazaki et al. The following value provided the best fit

$$\Sigma_{av} = 230 \text{ cm}^{-1}.$$

This value was then used to compare the power density factors (see definition in Section 2) predicted by RAD_HEAT with those of the existing correlation in the code ELESIM/ELESTRES using the initial (original) and extended databases. The case was that of a single uranium oxide rod of 12.15 mm in diameter with an enrichment of .71% and burnup of 400 MWh/kgU. The rod was immersed in D_2O . Cross sections used in this calculation were those associated with the outer pins of a 37-pin CANDU bundle and were obtained from a WIMS-AECL calculation. Power density factors are shown in Figure 2 and Table 2 (columns 2, 3 and 4) as a function of normalized (fraction of pellet radius) radial position (column 1 of Table 2). In columns 5, 6 and 7 of Table 2 we give the percentage difference between the three sets of power density factors: RAD_HEAT versus the initial (% rad-*ini*) and extended (% rad-*ext*) databases, and the initial versus the extended database (% *ini-ext*). The code CE-HAMMER could divide the fuel pin in at most 10 regions, while we have been using RAD_HEAT with over a thousand mesh points. The effect of a coarser mesh is to average the power density over a larger annulus, therefore decreasing its value, especially in the vicinity of the surface where the variation of the resonance capture rates is the greatest. This would explain why the difference between the power density factors calculated by RAD_HEAT and those evaluated by the existing correlation in ELESIM/ELESTRES is greater near the surface of the fuel pin, since the correlations are based on fitting CE-HAMMER calculated values.

It is important to notice that the same value of Σ_{av} has been used to model different types of fuel (metal or oxide, different radii and burnup). Although further tests are required to confirm the universality of this parameter, Wagner's comparison with Hellstrand's

experimental data [4] suggests that this might be the case. Work done by P.G. Boczar (private communication 1987) on resonance capture also suggests the universality of Σ_{av} .

6. CONCLUSION

Presently there are two databases available to calculate the local heat generation rate using the code ELESIM/ELESTRES. Although both databases have been derived from CE-HAMMER runs, and the function used for fitting its results is the same, there are noticeable differences (see column 7 of Table 2) in applying the two databases. The source of the problem has never been thoroughly investigated (it is believed that differences in fitting procedures are the main cause) but a solution to this problem is clearly needed. This was the main motivation behind our efforts to develop a more mechanistic approach to the evaluation of the local heat generation rate in a fuel pin. In ELESIM/ELESTRES, the resonance capture phenomenon is not modeled explicitly. The benefit of explicitly calculating neutron capture rates by U^{238} gives the possibility of validating the code using existing experimental data on such capture rates. Further tests of RAD_HEAT will include comparisons with Hellstrand's experimental data [4] on resonance capture by U^{238} .

Acknowledgments

We are grateful to S. Douglas, J. Griffiths and P. Laughton for many helpful discussions on the topics related to this work and for assistance in the use of WIMS-AECL. We are indebted to P.G. Boczar, A. Okazaki, D.W. Hone and D.F. Allen, whose previous work in this area has been used by us in the present study.

References

1. M.J.F. Notley, "ELESIM: A Computer Code for Predicting the Performance of Nuclear Fuel Elements," Nuclear Technology, Vol. 44, p.445, 1979 August.
2. H.H. Wong, E. Alp, W.R. Clendening, M. Tayal and L.R. Jones, "ELESTRES: A Finite Element Fuel Model for Normal Operating Conditions," Nuclear Technology, 57, 1982 May, 203-212.
3. M. Wagner, "Spatial Distribution of Resonance Absorption in Fuel Elements," Nuclear Science and Engineering, Vol. 8, p.278, 1960.
4. E. Hellstrand, "Measurements of Neptunium Activity in Irradiated Uranium Rods," Proceedings of the Brookhaven Conference on Resonance Absorption of Neutrons in Nuclear Reactors," p. 32, 1956 July.

Table 1: Relative Total Neutron Capture Rate in U^{238}

distance (cm)	ZEEP	RAD_HEAT	% difference
0.200	0.096	0.098	-1.75
0.239	0.105	0.098	6.54
0.298	0.106	0.098	7.69
0.400	0.099	0.099	0.56
0.503	0.109	0.100	8.25
0.604	0.119	0.101	15.66
0.707	0.130	0.102	21.66
0.808	0.120	0.104	13.44
0.892	0.115	0.106	8.47
1.012	0.124	0.108	12.65
1.114	0.127	0.112	11.94
1.213	0.123	0.117	5.34
1.215	0.124	0.116	6.99
1.307	0.135	0.122	9.12
1.308	0.134	0.122	8.39
1.419	0.140	0.133	4.79
1.5156	0.159	0.153	1.01
1.5157	0.155	0.154	3.78
1.573	0.175	0.190	-8.38
1.596	0.239	0.224	6.12
1.611	0.255	0.283	-10.96
1.612	0.275	0.287	-4.24
1.617	0.289	0.316	-9.41
1.621	0.341	0.386	-13.31
1.624	0.456	0.462	-1.36
1.630	1.000	1.000	0.00

Table 2 : Relative Power Density Factors

frac. rad.	rad_heat	ext. tab.	init. tab.	%rad-ini	%rad-ext	%init-ext
0.05	0.892	0.9	0.851	4.83	-0.88	5.76
0.308	0.900	0.912	0.864	4.18	-1.30	5.56
0.442	0.910	0.924	0.879	3.50	-1.54	5.12
0.543	0.921	0.936	0.892	3.21	-1.64	4.93
0.628	0.933	0.948	0.907	2.88	-1.57	4.52
0.704	0.948	0.959	0.922	2.83	-1.13	4.01
0.771	0.967	0.975	0.939	2.94	-0.86	3.83
0.834	0.995	0.995	0.967	2.88	-0.01	2.90
0.892	1.039	1.04	1.045	-0.55	-0.07	-0.48
0.946	1.121	1.16	1.262	-11.15	-3.34	-8.08
0.957	1.156	1.204	1.352	-14.53	-4.03	-10.95
0.967	1.204	1.255	1.447	-16.81	-4.08	-13.27
0.977	1.280	1.316	1.579	-18.93	-2.73	-16.66
0.987	1.449	1.388	1.75	-17.18	4.42	-20.69
0.992	1.634	1.42	1.82	-10.20	15.10	-21.98
0.997	2.048	1.46	1.89	8.36	40.27	-22.75

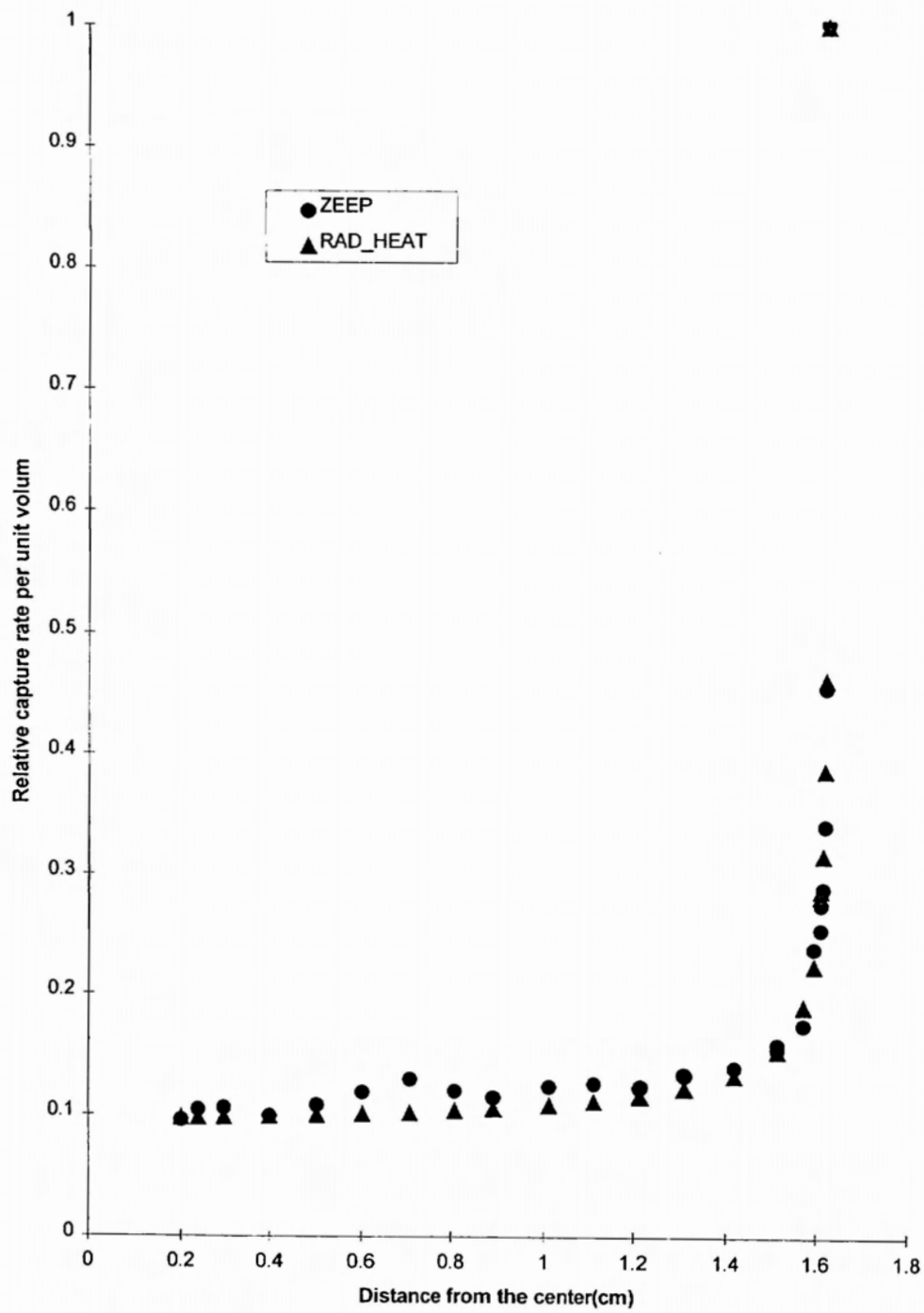


Fig. 1 Relative total neutron capture rate

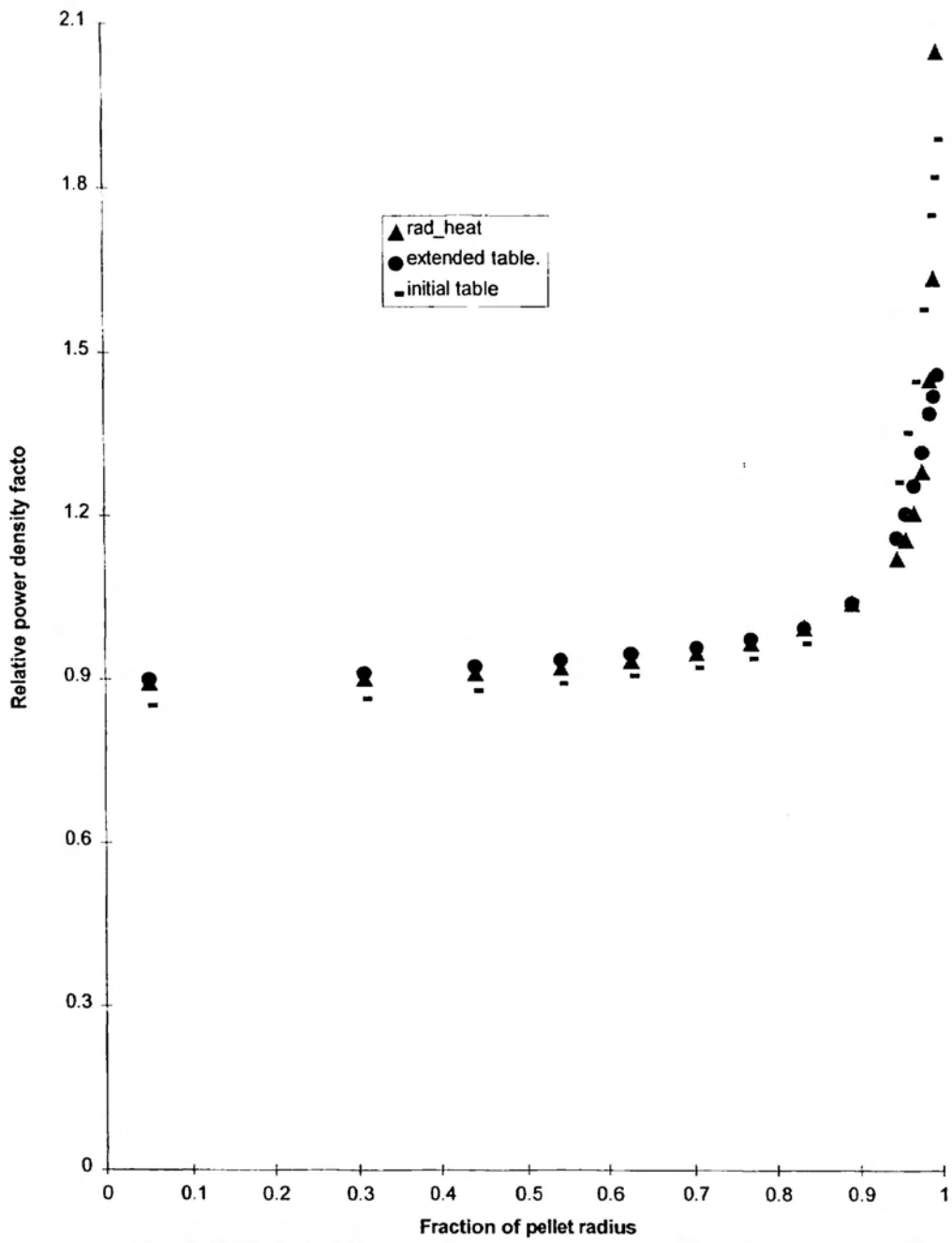


Fig. 2 Radial profile of relative power density factor for a burnup of 400 MWh/kgU